Evidence of rising groundwater and potential for sustainable management amid multi-year droughts in the pastoral regions of northern Kenya

Denis Macharia Muthike [1*], Styvers Kathuni [2], Christian Muragijimana[3], Taylor Sharpe [1], Gabriel Senay [4], Evan Thomas[1]

1 Mortenson Center in Global Engineering & Resilience, University of Colorado Boulder, 4001 Discovery Drive, Boulder, 80303, CO, USA
2 Millennium Water Alliance, Nairobi, Kenya
3 Virridy, Boulder, CO, USA
4 Earth Resources Observation & Science Center, United States Geological Survey, Fort Collins Science Center, Fort Collins, CO, USA

* denis.muthike@colorado.edu

*

Abstract Groundwater underpins water security in the drylands of East Africa, where climate extremes and increasing groundwater use pose growing water management challenges. This study examines groundwater dynamics in arid northern Kenya using multi-source data that combine in-situ electronic sensor measurements with satellite-based rainfall observations, terrestrial water storage anomalies, and model simulations of groundwater storage. Analysis of long-term rainfall records reveals pronounced hydroclimatic variability over the past four decades. The analysis revealed a clear climate signal in regional water storage, characterized by pronounced interannual variability driven by alternating drought and wet extremes during the long rains (March–May; MAM) and the short rains (October–December; OND) seasons. The OND season showed a progressive tendency toward wetter conditions over the study period, while MAM rains experienced episodic wet anomalies. Groundwater storage increased gradually from 2004 to 2024, with notable declines during multi-year droughts and strong rebounds during wet periods. Annual mean groundwater storage across the study domain over the same period increased by approximately 21.7%, rising from 109.68 km^3 to 133.49 km^3. At the well scale, monitored sites exhibited distinct drawdown–recovery behavior and delayed responses to cumulative rainfall, with lags ranging from approximately one to four months. Differences among sites highlight the heterogeneous nature of groundwater responses across the region and are likely influenced by local hydrogeologic controls. Recovery ratios suggest that, during the monitoring period, short-term abstraction was generally offset by recovery, findings that could support evidence of potential groundwater sustainability. Overall, these findings demonstrate the value of high-frequency groundwater monitoring and satellite observations for diagnosing groundwater dynamics in data-scarce drylands and emphasize the need for sustained monitoring and improved hydrogeological characterization to support groundwater management under intensifying climate variability and rising water demand.

Introduction

Groundwater is the primary reliable water source for pastoral livelihoods in arid and semi-arid regions of the Horn of Africa [1–3]. This region is characterized by low and highly variable rainfall, limited surface water storage, and recurrent droughts [4], conditions that elevate the strategic importance of groundwater for domestic, livestock, and livelihood needs. Despite groundwater's centrality to water security, a quantitative understanding of its dynamics in this region remains limited. Drilling has expanded rapidly to meet humanitarian and development needs, often in data-poor contexts where aquifer properties are poorly known, pumping is weakly regulated, and monitoring networks are sparse. As a result, decision-makers face a recurring challenge: balancing urgent water-supply objectives with long-term groundwater viability amid intensifying climate variability and demand. While many global assessments indicate unsustainable groundwater extraction [5,6], recent analyses suggest that parts of sub-Saharan Africa have experienced stable or rising groundwater storage [7].

Prevailing environmental conditions influence human-driven groundwater drawdown and natural recovery in northern Kenya [1,8]. The balance between the amount of water withdrawn from groundwater aquifers and the aquifers' ability to rebound following rainfall and abstraction effects has profound impacts on the short- and long-term sustainability of groundwater resources in this region. Abstractions at a rate that exceeds natural recharge can prolong groundwater recovery [9], reduce streamflows [10], compromise the health of groundwater-dependent ecosystems [11], and impact long-term water storage [12].

Increased abstractions have been shown to correlate with dry conditions. Thomas et al. [1] found that well use in northern Kenya increased by over 20% following weeks of no rainfall compared to weeks preceded by some rainfall. In a slightly different setting in southern Kenya, but where the rural population is primarily dependent on groundwater, Thomson et al. [13] found a similar association, with groundwater pump use reduced by 34% in the wet season compared to the dry season. Taken together with aquifer storage and climate interactions, the clear link between environmental variability and groundwater use places groundwater sustainability at the center of planning for water resources in the region as humanitarian agencies, county and national governments intensify groundwater development as a drought adaptation intervention [2].

Data-driven decision-making opportunities for groundwater governance in northern Kenya are limited. Policymakers and development partners lack the necessary monitoring data and modeling tools to make informed choices. While significant efforts have been made to improve the evidence base upon which groundwater development can be founded, water level records – often instantaneous and infrequent– are still limited to a small subset of wells. Additionally, metadata on well construction (e.g., well completion reports), hydrogeology, and pumping rates are often incomplete, inaccessible or outdated. Planning and operational decisions such as well siting, pump sizing and schedules, allocation rules during drought, and investment in storage or recharge enhancement are frequently made without explicit consideration of data-informed aquifer responses. Wells are commonly sited opportunistically (e.g., proximity to settlements or infrastructure) rather than with systematic evaluation of hydrogeologic prospects, connectivity to recharge zones, or impacts of neighboring abstractions. At the site level, abstraction practices rarely reference measured water-level trends or recovery rates. At the regional scale, allocation across sectors (i.e., domestic, livestock, smallholder irrigation, and institutions) seldom accounts for externalities where pumping in one area can depress groundwater levels elsewhere. These gaps can heighten the risk of chronic declines [14] and well failures during drought, with lasting outcomes including conflict over unreliable sources.

The National Drought Management Agency (NDMA) oversees the program on "Ending Drought Emergencies in Kenya", whose goal is to identify and manage strategic wells critical for water provision to people and livestock during severe drought periods [1,2]. This program has increased drought resilience by focusing resources on these strategic wells across northern Kenya. But little is known about the sustainability of these sites, and decisions about which wells are identified as strategic or not rarely reference empirical evidence about the health of the groundwater. Prioritization is dependent on anecdotal evidence, such as livestock movement routes, which can change over time due to environmental and socio-political factors. NDMA's programs can be strengthened by research that generates evidence on the state of groundwater health, which in turn can support data-informed prioritization and focus resources to support drought resilience.

Against this backdrop, this study integrates high-frequency in situ groundwater level observations from four community wells in Turkana with satellite-derived rainfall and terrestrial water storage to characterize short-term site-level groundwater and regional terrestrial water storage dynamics under rainfall variability and abstraction. A process-based approach was adopted to quantify drawdown and recovery behavior, estimate representative groundwater heads during non-pumping periods, and examine lagged relationships between cumulative rainfall and groundwater response. In addition, the study used modeled groundwater storage to investigate temporal trends in annual groundwater storage across the study domain. As a result, the study aims to provide decision-relevant insights into groundwater behavior in the region, while recognizing the limitations of both short observational records and coarse satellite products used in the study.

Materials and Methods

Water level data

This study was located in Turkana (Fig. 1), a region in northwestern Kenya comprising drylands that support the livelihoods of pastoralist populations. The climate in this region is arid with annual rainfall ranging between 200–500 mm. Annual rainfall follows a bimodal pattern with rainfall peaks in April during the boreal spring season (long rains: March–May or “MAM”) and November during the boreal autumn season (short rains: October–December or “OND”). There is a long dry season between June–September; however, data records show some rainfall is also received in July in the western region, including some parts of western Turkana. Annual mean temperatures range from 20–40 degrees Celsius with high evapotranspiration throughout the year [15].

Water level data were collected from four community groundwater abstraction wells. These wells are representative of the groundwater supply systems in Turkana and the larger northern drylands. The wells have motorized pumps powered by solar energy (Fig. 2) that extract water to elevated tanks that supply community water points or, in some cases, household networks. Like others across this dryland region, these motorized wells are the primary reliable source of water for domestic, livestock, and small irrigation uses. They are managed primarily by the local communities in partnership with local water services and humanitarian organizations [1].

The Kalobeyei community well site is located in the Kalobeyei alluvial system comprising clayey alluvium overlying Tertiary lavas, with sand lenses being present in proximity to the major lagas [16]. This site is within the larger Kakuma refugee camp complex and serves the host community and the integrated refugee population. Kakemera, Nadapal-IRC, and Loturerei sites are within the larger Lodwar alluvial aquifer system serving the rural communities surrounding Lodwar town. The Lodwar aquifer comprises shallow, intermediate, and deep aquifers that are replenished through diffuse recharge by the Turkwel River and Kawalase River during the wet season, as well as direct infiltration during rainfall events [17]. The reported drilled well depths are 77 m, 98 m, 60 m, and 112 m for Kakemera, Nadapal-IRC, Loturerei, and Kalobeyei, respectively. The reported flow rate for Kakemera and Kalobeyei is 20 m^3/hr, while Nadapal-IRC and Loturerei have a flow rate of 8 m^3/hr. Kakemera, Kalobeyei, and Nadapal-IRC are categorized as strategic wells and form part of a large network of wells critical for water provision during drought periods for people and livestock. This strategic well network is overseen by the National Drought Management Agency (NDMA) as part of the national ”Ending Drought Emergency” program [2, 8].

Water level data were collected using the satellite-connected Holykell HPT604-A submersible water level pressure transducers. These sensors have a measurement error of $\leq \pm 0.5\%$ of their full scale and a custom range level of 50 cm–500 m. The sampling frequency was set at 15 minutes (Fig. 3), resulting in 1532 total unique days of observations across the four sites [range: 269–486]. Sensor installations were done between May and July 2023. Sensors were installed to correspond to the level of submersible well pumps; thus, water levels were interpreted as water column height above the sensor, not as depth-to-water. Higher (lower) values therefore indicated a rising (falling) groundwater level. For interpretation, drawdown and recovery refer to a reduction and increase in the water-column height, respectively. Water level pressure transducers were installed at depths of 57 m, 63 m, 48 m, and 80 m in Kakemera, Nadapal-IRC, Loturerei, and Kalobeyei, respectively. Data collection periods varied across sites due to intermittent disruptions, including sensor malfunctions and the permanent loss of satellite connectivity following the discontinuation of the Swarm Technologies satellite network in November 2024.

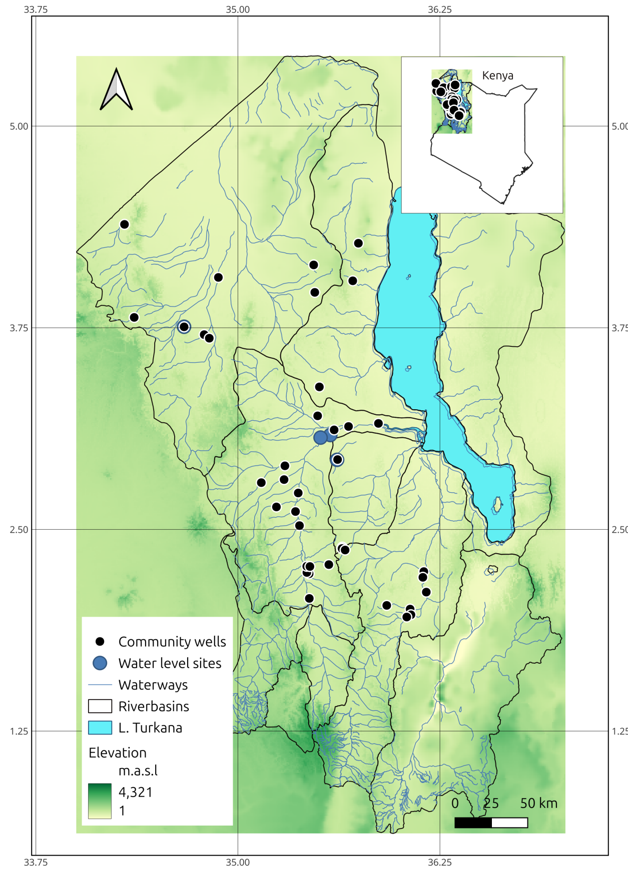

Fig 1. Locations of water level sensor installations at groundwater well sites (blue dots) in Kakemera, Kalobeyei, Loturerei, and Nadapal-IRC in Turkana, Kenya. The four sites are representative of the typical community well systems in this region. They are motorized wells using solar, diesel or hybrid power supply systems, and serve as the primary water sources for domestic, livestock, and small irrigation schemes in the dry season. Elevation classes provide the local topographical context, whereas the black lines are the major river basins in the Turkana region. The light blue polygon shows the extent of Lake Turkana.

Remote sensing data

Two satellite-based gridded observational datasets of rainfall and terrestrial water storage (TWS), and model simulations of groundwater storage (GWS) were used in this study to map recent seasonal extreme rainfall events and the response in terrestrial water storage comprising both surface and groundwater. Daily and monthly rainfall data were sourced from the Tropical Applications of Meteorology Using Satellite Data and Ground-Based Observations (TAMSAT) v3.1 product [18–20] downloaded from the International Research Institute for Climate and Society's Climate Data Library [`https://iridl.ldeo.columbia.edu/SOURCES/.Reading/.Meteorology/.TAMSAT/.v3p1/`] [21]. This dataset spans the period 1983—present, covering the African continent at daily, dekadal, and monthly timesteps. The data are provided as gridded files at a spatial resolution of 0.0375° (approximately 4 km at the equator). Studies have validated this dataset in Sub-Saharan Africa, finding it reliable for climate research in Africa with a validated wet bias of 12% compared to rain gauge measurements at the monthly time step and 11% at the daily time step [22].

Monthly estimates of terrestrial water storage were sourced from the Gravity Recovery and Climate Experiment (GRACE) mascon data provided by the Jet Propulsion Laboratory (JPL) [23]. The regionally averaged data were downloaded from the GRACE Data Analysis Tool

Fig 2. An example of a motorized community well site infrastructure in Turkana, Kenya, showing the well in the middle, solar panels for water pumping, and the pump control room.

[https://grace.jpl.nasa.gov/data-analysis-tool/]. This dataset includes estimates from GRACE and GRACE Follow-On missions, both of which infer terrestrial water storage from gravity measurements. The data are provided as 50 by 50 km grids, represent spatial and temporal terrestrial water anomalies, and incorporate surface, groundwater storage, including snow/ice and soil moisture. For this study, terrestrial water represents surface and groundwater storage, with the latter representing a major proportion of the anomalies due to the ephemeral nature of the surface water in the region [24]. The GRACE/GRACE-FO products have been widely adopted in water balance studies in Africa [7, 25, 26]. They provide global coverage of terrestrial water storage observations essential for improving our understanding of Earth's freshwater availability and enable comparisons between regions. They have also been used to calibrate and validate groundwater models, helping uncover policy-relevant trends in drought risks and the sustainability of groundwater aquifers [12, 27, 28].

Modeled estimates of absolute groundwater storage were obtained from the NASA Global Land Data Assimilation System version 2.2 (GLDAS) through the NASA Earthdata repository. This product includes spatially and temporally downscaled, and vertically disaggregated GRACE data obtained through GRACE data assimilation into the Catchment Land Surface Model (CLSM) within the Land Information System (LIS) [28]. The daily "GWS_tavg" product provided at a 0.25° grid resolution, was utilized, and monthly and annual mean GWS were subsequently computed. Both GRACE and GLDAS estimates were incorporated in this study because the Turkana region includes Lake Turkana, which potentially masks the groundwater storage signal in the GRACE TWS data due to the coarse resolution of this product. The goal, therefore, was to use the GLDAS-CLSM estimates as a separate indicator of groundwater-specific changes during the study period.

Estimating well drawdown and recovery

A statistical framework was developed in `R` version 4.3.3 [29] to analyze groundwater dynamics using the high-frequency water level pressure transducer data. Because the well sites lack hydrogeological characterizations required for recharge calculations, a data-driven approach was employed to quantify drawdown and recovery, and to investigate the associations between rainfall and representative groundwater heads during recovery periods. The four well sites experience regular pumping varying from 6–10 hrs/day. Recovery periods were therefore identified from continuous rising segments in the time series following observed drawdown cycles, consistent with field-reported pump-off periods. A visual inspection of the hydrographs in Fig. 3 confirmed that these periods corresponded to non-pumping hours reported by the corresponding well operators.

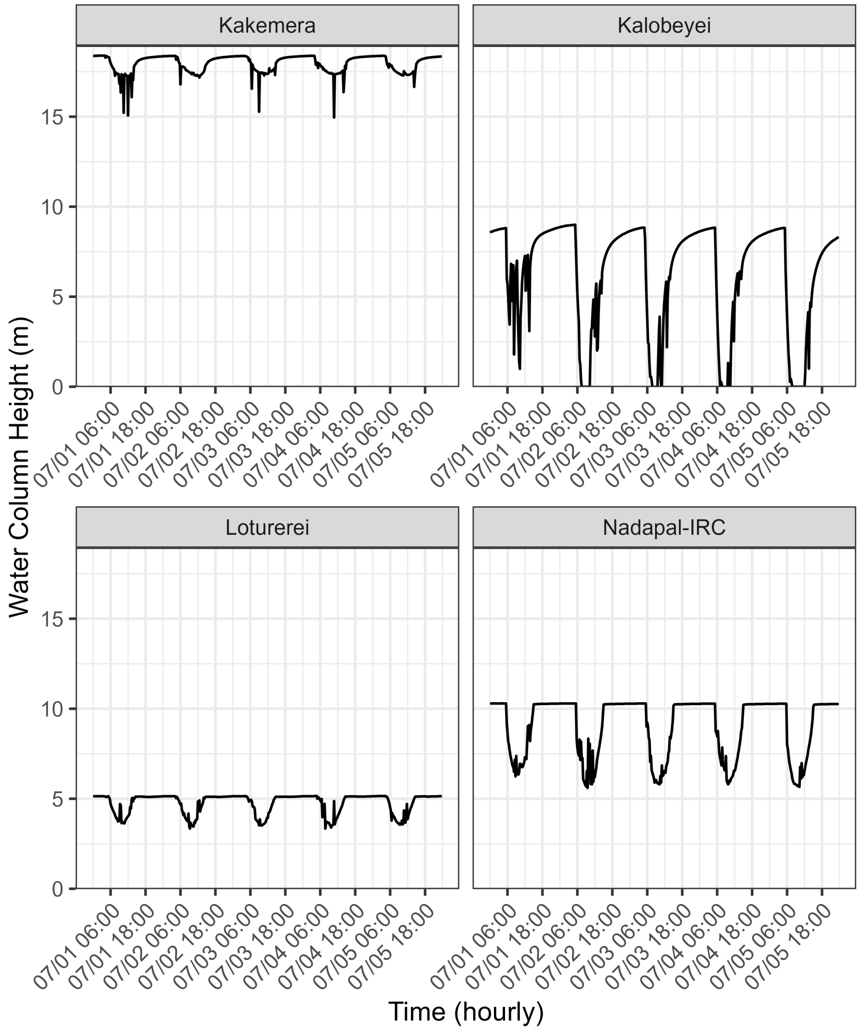

Fig 3. Sample 15-minute water level measurements for the four study sites showing declining and recovering water levels as measured by the water level pressure transducers. The reported water level is the water column height relative to the sensor installation depth. The x-axis is set to a common scale for between-site visual comparisons.

Data pre-processing

Pressure transducer water level time series data underwent rigorous pre-processing to ensure data integrity. Duplicate timestamps were identified and resolved by retaining the observation closest to the local rolling median of surrounding data points within a 1.5-hour window, mitigating spurious spikes while preserving data continuity. A complete 15-minute timeline was constructed spanning the entire period of record for each site, with observed data aligned to this consistent temporal framework without interpolation, and missing data assigned the label “NA”. This explicit representation of missing values maintained consistent spacing and prevented artificial temporal compression, ensuring that water level differences were computed over true 15-minute intervals.

With cleaned water level data, continuous periods of valid observations were delineated through segmentation, where new segment labels were assigned whenever missing data interrupted the series. This segmentation strategy prevented miscalculation of water level differences across data gaps. For each continuous segment, incremental water level changes Δh were computed as differences between consecutive 15-minute readings (Eq. 1):

$$\Delta h_i = h_i - h_{i-1} \tag{1}$$

where h_i is the water column height (m) at the i-th 15-minute timestamp and h_{i-1} is the preceding observation within the same continuous data segment. Differences spanning data gaps are excluded by the segmentation procedure.

Daily and weekly drawdown and recovery

The Δh values served as the basis for quantifying aquifer flux dynamics. Recovery was defined as the sum of all positive Δh values, indicating a rising water column, and drawdown as the sum of absolute negative Δh values, representing a falling water column. Total daily recovery R_d and drawdown D_d (m day^{-1}) were calculated by summing positive and absolute negative increments (Eq. 2 and 3) within each calendar day d, respectively:

$$R_d = \sum_{i \in D} \max(\Delta h_i,\ 0) \tag{2}$$

$$D_d = \sum_{i \in D} |\min(\Delta h_i,\ 0)| \tag{3}$$

where D is the set of all valid 15-minute intervals within calendar day d. Weekly aggregation was chosen to balance temporal precision and noise reduction, allowing comparison across sites with occasional data gaps, while retaining sufficient resolution to capture pumping and recovery cycles [1]. Weekly totals were obtained by summing the daily values over each calendar week.

*

Well recovery ratio

Well recovery ratios (Eq. 4) were calculated by dividing total cumulative recovery by total cumulative drawdown over the monitoring period:

$$\rho = \frac{\sum_{w} R_w}{\sum_{w} D_w} \tag{4}$$

A ratio $\rho > 1$ implies net positive aquifer storage, whereas $\rho < 1$ implies an aquifer experiencing more drawdown than recovery can offset. A value of $\rho = 1$ implies a balance between abstraction and recharge.

*

Rainfall–groundwater lag correlation To investigate the associations between daily peak water column and rainfall, daily groundwater head levels reflective of aquifer equilibrium conditions were estimated using a targeted approach focused exclusively on recovery periods. The 95$^{\text{th}}$ percentile of head values during recovery periods was computed for each qualifying day (Eq. 5):

$$\hat{h}_d = P_{95}(\{h_i : i \in R_d\}) \tag{5}$$

where R_d is the set of all 15-minute observations recorded during recovery periods on day d, and $P_{95}(\cdot)$ denotes the 95$^{\text{th}}$ empirical percentile. This statistic represents the upper envelope of water column levels achieved during aquifer rebound, minimising noise and short-term pressure surges while approximating the quasi-equilibrium head. Sensitivity tests using the 90$^{\text{th}}$ and 99$^{\text{th}}$ percentiles showed less than 1% variation in results.

Rainfall–groundwater relationships were quantified using Pearson correlation coefficients between the daily groundwater head and cumulative antecedent rainfall totals computed over accumulation windows of 10, 15, 30, 60, 90, and 120 days (Eq. 6 and 7):

$$P_l(d) = \sum_{k=0}^{l-1} P(d-k) \tag{6}$$

where $P(d)$ is the daily rainfall (mm) on day d. The Pearson correlation at lag l is:

$$r(l) = \frac{\sum_d \left(\hat{h}_d - \bar{\hat{h}}\right)\left(P_l(d) - \bar{P}_l\right)}{\sqrt{\sum_d \left(\hat{h}_d - \bar{\hat{h}}\right)^2 \cdot \sum_d \left(P_l(d) - \bar{P}_l\right)^2}} \tag{7}$$

where $\bar{\hat{h}}$ and $\bar{P}_l$ are the respective sample means over all qualifying days. The dominant recharge response time at each site was identified as the lag l^* at which $r(l)$ reaches its maximum. Peak correlation coefficients were interpreted as indicative of dominant recharge response times.

Extreme climate events and terrestrial water storage

Gridded climate data were processed and analyzed using both R and the Climate Data Operators; a tool for managing gridded timeseries climate data stored in Network Common Data Form (NetCDF) files [30]. We computed seasonal rainfall anomalies, expressed as a percentage of climatological means, for the two main seasons: March–May [MAM] and October–December [OND]. The period of analysis was 1983–2024, upon which seasonal climatological means were calculated at a grid level and later aggregated over the Turkana region shown in Fig. 1. Seasonal (3-month) gridded standardized anomalies (Z-scores) [31, 32] were computed for each year in the climatology, and the frequency of dry and wet events was calculated from the seasonal Z-scores data. We classified dry events as Z-score values ≤ -0.8 and wet events as Z-score values ≥ 0.8. We then summed all dry and wet events at the grid cell level as an indicator of spatial-temporal exposure to extreme events. GRACE terrestrial water storage anomalies and GLDAS groundwater storage estimates were averaged over the same region for further analysis. We interpreted the GRACE data as reflecting regional context rather than site-specific changes in groundwater storage.

Monthly and mean annual groundwater storage volume (km^3) were computed from the Global Land Data Assimilation System Version 2.2 (GLDAS-2.2) Catchment Land Surface Model (CLSM) monthly output for the period 2004–2024. The groundwater storage variable (GWS_tavg), which represents absolute groundwater storage in millimeters of equivalent water depth, was extracted for each grid cell within the study domain. Monthly groundwater storage volume per cell was obtained by converting GWS_tavg from millimeters to kilometers and multiplying by the cell area. The total domain-wide groundwater volume for each month was computed by summing across all valid grid cells within the study domain. Annual mean groundwater volume was calculated by averaging the 12 monthly totals for each calendar year, yielding a time series of annual mean groundwater storage volume (km^3) over the 21-year period.

A monthly standardized groundwater storage index (SGSI) was also computed using the volumetric monthly groundwater storage time series data to assess groundwater storage evolution under drought and pluvial conditions. We adopted an approach analogous to the Standardized Precipitation Index [33]. For each calendar month, a two-parameter gamma distribution was fitted to the historical distribution of domain-wide volumetric groundwater storage via maximum likelihood estimation, and the resulting cumulative probabilities were transformed to standard normal quantiles to yield a dimensionless index with zero mean and unit variance. This approach mirrors the parametric SPI formulation in that it removes the seasonal cycle implicitly through within-month fitting, produces a normally distributed index amenable to threshold-based drought classification, and remains applicable to future observations outside the calibration period without requiring re-ranking of the historical record; advantages over non-parametric alternatives when the observational record is of moderate length [34].

Results and Discussion

Recent extreme climate events

The analysis of seasonal rainfall anomalies and extreme event frequencies revealed distinct spatial and temporal patterns across the study domain during both MAM (long rains) and OND (short rains) seasons from 1983–2024 (Fig. 4 and Fig. 5). The MAM season exhibited considerable interannual variability characterized by alternating drought and extreme wet conditions. Spatial analysis revealed that droughts (Z-score ≤ -0.8) were more frequent and spatially extensive during MAM, particularly across central and southern regions where drought seasons occurred up to 33–38% in the 42-season climatology (Fig. 5). This pattern indicates a persistent tendency toward below-normal rainfall during the long rains, consistent with published literature [35, 36].

Temporally, the MAM season showed marked fluctuations between extreme conditions. The year 2010 featured generally normal to wet conditions across most of the region (Fig. 4). In contrast, 2011 marked a severe drought episode, affecting the entire region, consistent with the documented Horn of Africa drought in 2010/2011 [37]. More recent MAM seasons (2018, 2020, 2023) showed predominantly wet anomalies, especially pronounced over central and southern areas. The OND season had a notable evolution toward wetter conditions, with distinct spatial characteristics. Similar to the MAM wet patterns, OND wet events (Z-score ≥ 0.8) were spatially widespread and frequent, reaching up to 33% occurrences in the central and western regions (Fig. 5). OND droughts were concentrated mainly in central and southeastern areas, with relatively fewer events in the north. Widespread dry conditions were experienced in 2005 and 2010, with substantial negative anomalies across much of the region. A marked transition occurred in 2011, which exhibited strong wet anomalies, particularly concentrated in central regions. This wetting pattern persisted through 2015 and 2019, with anomalies exceeding 2-3 times the average values, reflecting intensified short rains during those years and consistent with studies examining the flood extremes in this region [38].

Our findings revealed two primary patterns of rainfall regime evolution in the Turkana region and its surrounding areas. First, OND rains became progressively wetter since 2011, representing a significant shift in the regional climate characterized by more frequent and widespread wet extremes. Second, MAM rains exhibited substantial interannual variability broadly dominated by drought conditions, featuring both extreme drought episodes (notably 2011) and pronounced wet anomalies (2018-2023). These spatial-temporal patterns align with documented regional climate shifts. The generally contrasting behaviors between seasons are consistent with broader regional trends linked to large-scale climate modes such as the El Niño—Southern Oscillation (ENSO) and the Indian Ocean Dipole [36, 38–41]. The observed changes have important implications for water resource management, and climate adaptation strategies in this vulnerable region, particularly given the differential impacts on the two primary rainy seasons. While these rainfall anomalies define the regional hydroclimatic forcing, their translation into groundwater recharge depends on site-specific subsurface properties and antecedent conditions, which are examined through well-scale response dynamics in the following section*s.

Trends in groundwater storage

Seasonal rainfall patterns exerted a notable influence on groundwater system behavior across the region. Terrestrial water storage, comprising both surface water and groundwater (Fig. 6), showed a consistent increase, with the largest gains occurring after the extremely wet conditions of 2019–2020 associated with a positive Indian Ocean Dipole event [38]. This increase persisted through the end of 2024, although storage declined substantially between late 2020 and early 2023. This decline coincided with five consecutive drought events following the anomalously wet MAM and OND seasons that preceded this period [42]. Storage began to rise again in 2024, corresponding with above-average MAM and OND rainfall in 2023 and 2024. Over the same period, modeled annual mean groundwater storage from GLDAS CSLM across the study domain increased by $\sim$21.7%, rising from 109.68 km^3 to 133.49 km^3.

Despite the generally rising trend in groundwater as shown in Fig 6a, the region's groundwater storage reveals a shift from predominantly negative anomalies prior to 2019, reflecting sustained below-normal storage conditions associated with recurrent drought episodes, to predominantly positive anomalies from 2019 onward. It appears that the 2019-2020 extreme rainfall conditions had a strong influence on the storage,

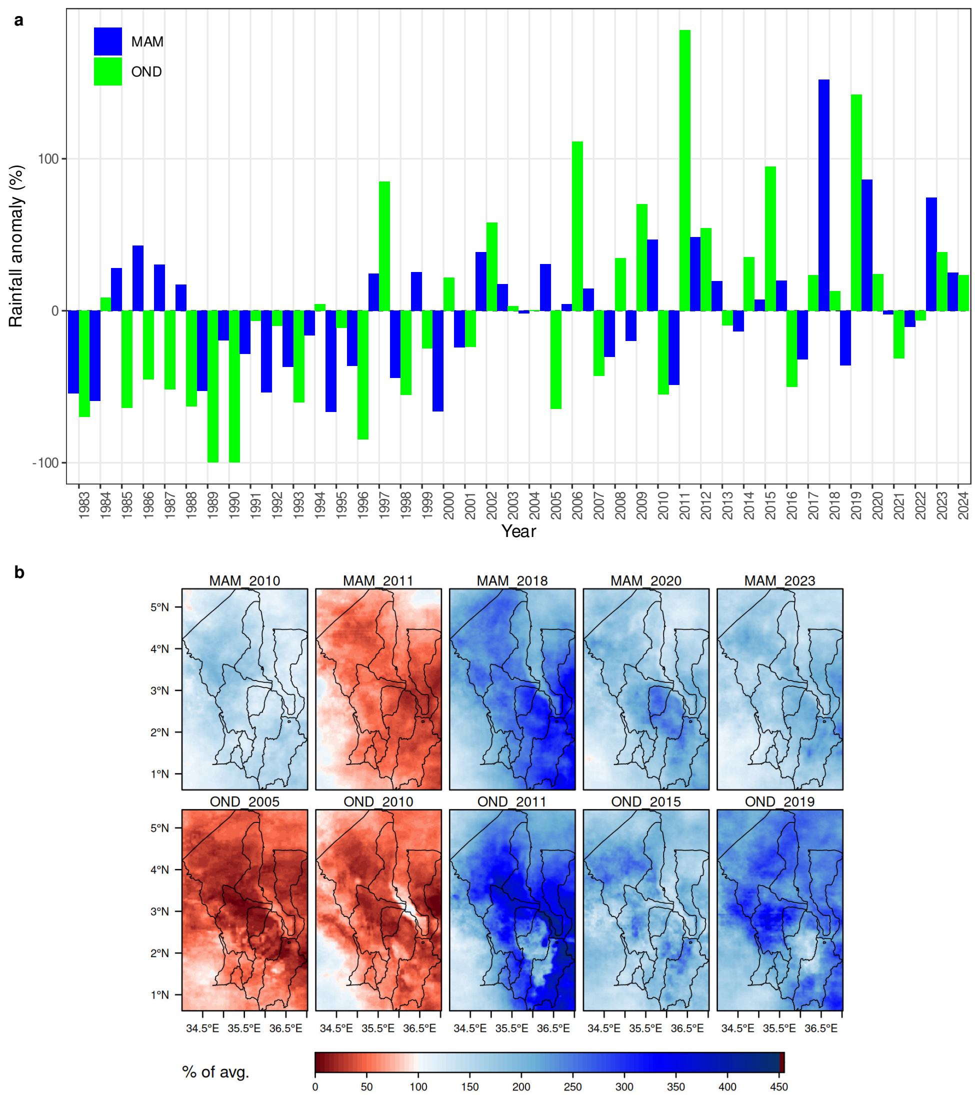

Fig 4. Seasonal rainfall anomalies across the Turkana region. The bar graph in **(a)** shows interannual anomalies for the March–May (MAM, blue) and October–December (OND, green) seasons from 1983–2024, expressed as percentage departures from the long-term seasonal mean, with zero indicating normal rainfall (dashed line). The maps in **(b)** show the spatial distribution of seasonal rainfall anomalies for selected dry or wet years across the region, where values below 100% (red) indicate below-normal rainfall and values above 100% (blue) indicate above-normal rainfall.

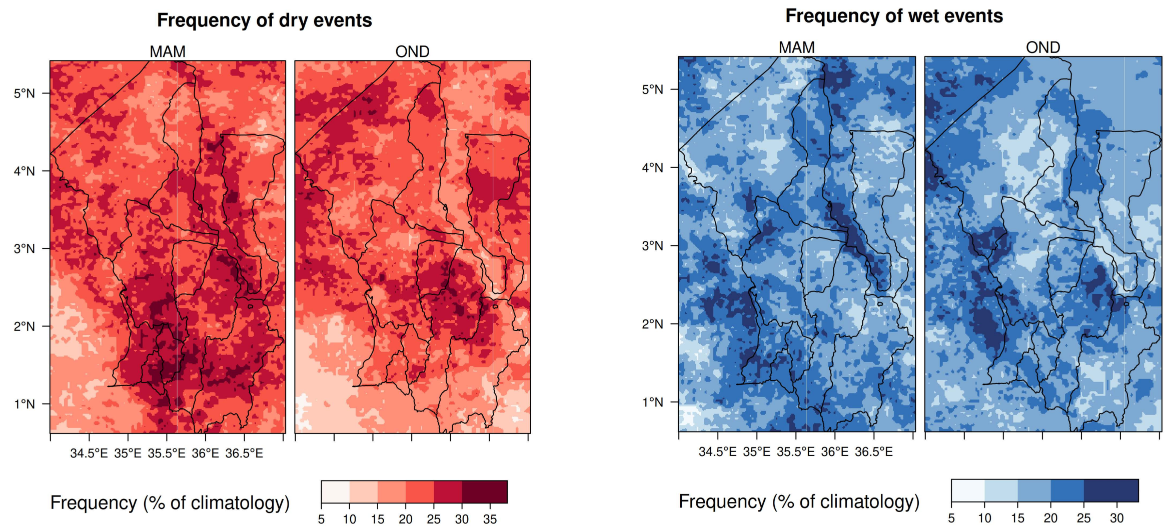

Fig 5. Maps of the frequency of dry and wet events over the period 1983-2024 for the March–May [MAM] and October–December [OND] rainy seasons. Dry and wet events are based on 3-month Standard Precipitation Index threshold of ≤ -0.8 and ≥ 0.8 for dry and wet events, respectively.

such that despite the consecutive failed rain seasons from October 2020 to early 2023 [42], the severity of these rainfall deficits was not greater than the gains from the 2019-2020 extreme rainfall for the groundwater storage to fall below the 21-yr climatological mean used to estimate the SGSI. The fluctuations in groundwater storage in response to prevailing rainfall conditions highlight the sensitivity of groundwater systems in the study region to climate extremes and reinforce the argument by [24] that groundwater storage changes in the region are strongly linked to anomalous rainfall events.

Well drawdown and recovery trends

Weekly groundwater fluctuations revealed distinct site-specific drawdown and recovery dynamics (Fig. 7). At Kakemera, frequent drawdowns of up to 10 m during late 2023 followed by lower-amplitude recoveries toward mid-2024 indicated sustained abstraction. The gradual stabilization in mid-2024 may have been due to a change to pumping conditions, an indication that water demand shifts after the generally good rains received in the region in the MAM season may have had a role in the observed abstraction trends. Kalobeyei exhibited the largest variations, with drawdowns exceeding 20 m and rapid recoveries of similar magnitude, consistent with intensive groundwater use and rapid recovery response to aquifer inflow. At Loturerei, smaller, symmetric fluctuations (± 4 m) reflected a system where extraction was consistently low and was well balanced with recovery. Nadapal-IRC showed a similar pattern as Loturerei but with larger extraction magnitudes (± 10 m).

Collectively, all the sites exhibited near-balanced drawdown–recovery behavior over the monitoring period, with recovery generally offsetting abstraction under prevailing climatic and operational conditions. A closer examination of net storage was taken into account for a better interpretation of this balance at each site. Mean weekly recovery ratios (recovery/drawdown) were 1.05 at Kalobeyei, 1.02 at Loturerei, 0.99 at Nadapal-IRC, and 1.03 at Kakemera, indicating near-balanced to slightly positive aquifer storage conditions. These ratios should be interpreted as short-term system behavior rather than long-term storage trends and reflect transient responses to abstraction and recent climatic conditions. Additionally, the observed rise in well heads and regional terrestrial water storage following major rainfall periods should be viewed as temporally consistent rather than causally linked; a finding that can be supported by detailed modeling of the groundwater in the study domain. The observed correspondence, therefore, provides a regional hydroclimatic context rather than validation of local groundwater storage change.

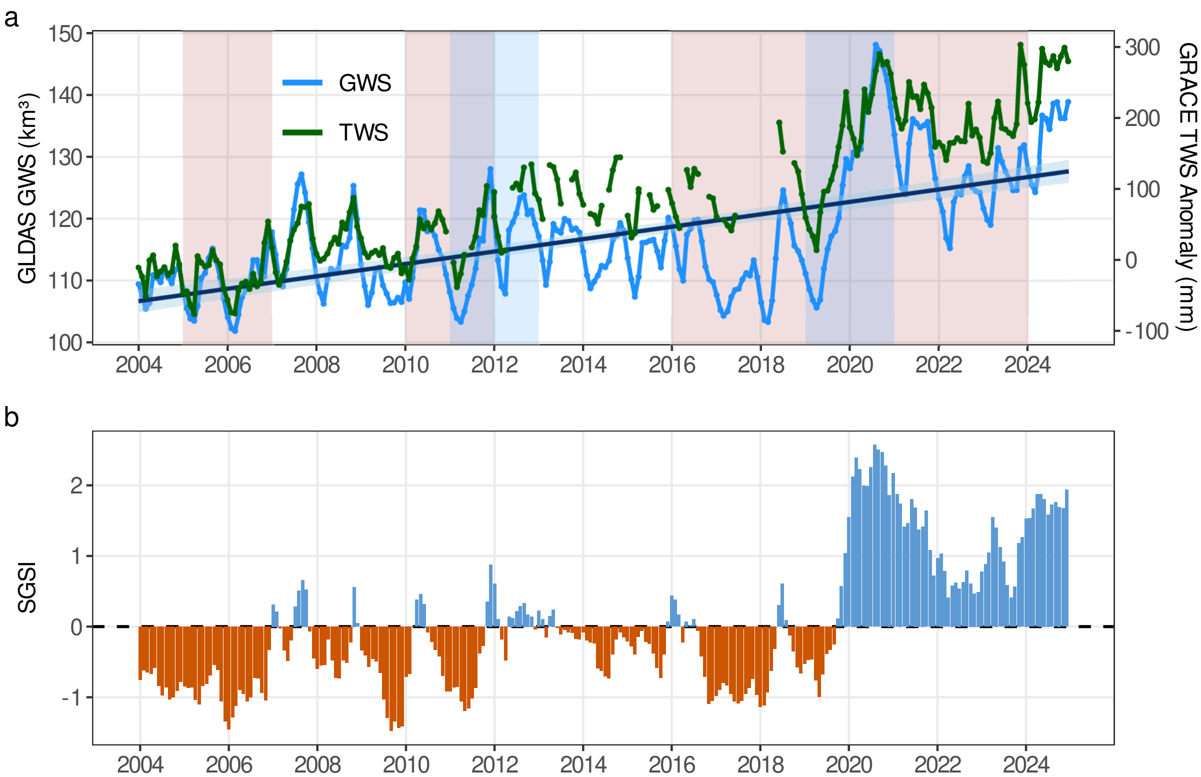

Fig 6. (a) Time series of groundwater storage estimated from the GLDAS Community Land Surface Model with GRACE data assimilation (blue, left axis) and terrestrial water storage (TWS) anomalies derived from GRACE/GRACE-FO satellite observations (green, right axis) for the study domain from 2004–2024. The dark blue line shows the linear trend in GLDAS groundwater storage, with the shaded band representing the 95% confidence interval. Brown vertical bands indicate major drought periods, while light blue bands indicate major flood periods. Both datasets exhibit substantial seasonal and interannual variability, with an overall increasing trend in groundwater storage over the study period. (b) Monthly Standardized Groundwater Storage Index (SGSI) computed from the GLDAS GWS volume time series over the same domain and period. Blue bars indicate positive SGSI values corresponding to above-normal groundwater storage, and orange bars indicate negative SGSI values corresponding to below-normal groundwater storage.

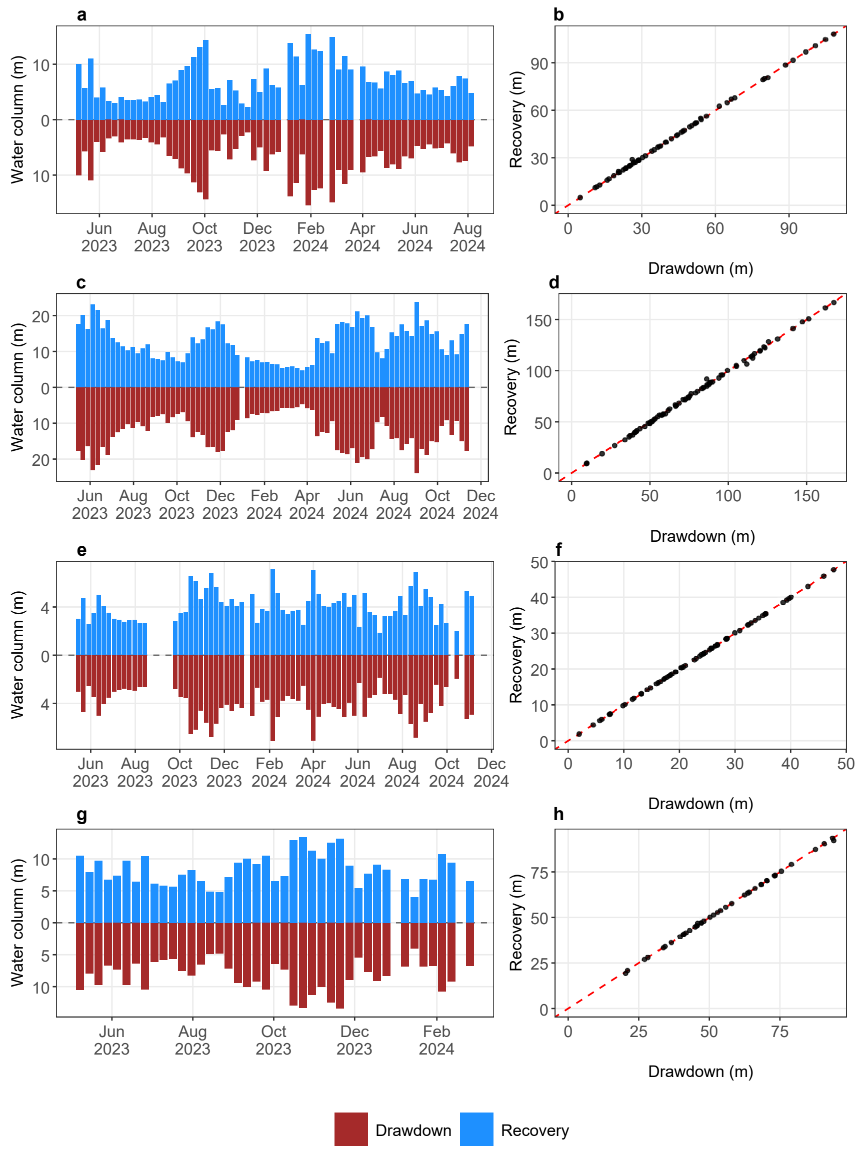

Fig 7. This figure visualizes the health of wells at the four sites by showing how much the water level drops after pumping ("drawdown") and how much it recovers during a rest period ("recovery") at the weekly time period. The graphs in the left panel show weekly mean water-column height variations, whereas the graphs in the right panel are scatterplots of the total weekly recovery and drawdown. The graphs correspond to the following sites: Kakemera (a,b), Kalobeyei (c,d), Loturerei (e,f) and Nadapal-IRC (g,h).

Associations between well recovery and rainfall

The lagged rainfall–groundwater correlations quantitatively support the visual patterns observed in the hydrographs of groundwater head (Fig. 8). All sites exhibited stronger and significant ($p < 0.001$) correlations with accumulated rainfall. Nadapal-IRC exhibited the highest observed rainfall–groundwater correlation within the monitoring period, with correlations rising sharply from $r = 0.29$ (15 days) and peaking at 90 days ($r = 0.93$). This may reflect a pronounced response to one or more recharge events. The pattern further suggests a delayed groundwater response consistent with relatively efficient hydraulic connectivity between recharge inputs and the monitored water level, although the absence of aquifer parameterization precludes direct inference of transmissivity or long-term storage capacity.

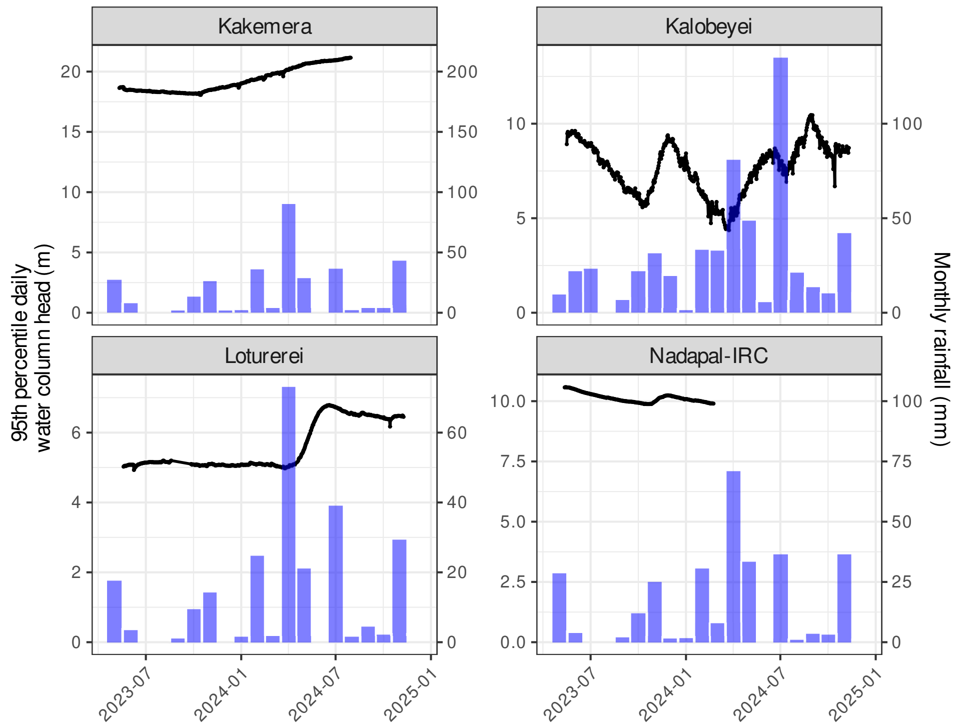

Fig 8. Site-level daily groundwater heads overlaid on TAMSAT monthly rainfall. Distinct rises in groundwater head at Kalobeyei and Loturerei closely follow major rainfall events, reflecting active recharge within shallow, permeable alluvial systems. In contrast, delayed responses at Kakemera and Nadapal-IRC could indicate aquifer systems where recharge transmission is slower. The site-specific patterns highlight variable hydrogeologic characteristics that mediate rainfall-groundwater coupling in the study sites.

Kalobeyei also displayed a robust response, with correlations strengthening steadily after 60 days ($r = 0.44$) and peaking at 120 days ($r = 0.65$). The lagged but significant increase suggests a generally efficient infiltration for a well-connected hydraulic system [16]. By contrast, Kakemera showed a modest correlation pattern with a peak at 90 days ($r = 0.44$), suggesting that recharge occurs gradually. It is important to note that, whereas this site is within the Lodwar Aquifer system [43] just like the Nadapal-IRC site, it is further away from the Turkwell river alluvial plain, which may explain the delayed and weaker correlations. Loturerei, though showing generally weak correlations ($r \leq 0.36$ at 120 days), maintained positive values, implying steady but low-magnitude recharge likely controlled by limited transmissivity.

Together, these patterns indicate that rainfall has a substantial and direct control on groundwater fluctuations in the Turkana region, but the timing and efficiency of recharge vary by site. The coexistence of both rapid and delayed recharge responses points to the need to consider aquifer characteristics when designing groundwater abstraction and monitoring strategies. This heterogeneity in groundwater response further underscores the vulnerability of groundwater systems in this region. Aquifer systems that recharge quickly during intense rainfall events offer immediate drought relief but can be more vulnerable to prolonged droughts.

Implications for groundwater management

The observed patterns of seasonal rainfall extremes and terrestrial water storage response reveal a hydrological system characterized by strong climate sensitivity and pronounced temporal variability in Turkana and the neighboring areas. The intensification of wet and dry extremes directly translated into observable impacts on the region's water storage dynamics, as revealed by GRACE terrestrial water storage trends and site-specific groundwater monitoring. The GRACE and GLDAS modeled terrestrial and groundwater storage trends demonstrated that sustained rainfall anomalies influenced variability in the hydrological cycles. Despite the major depletion events during the early 2000s to 2011 and 2020 to 2023, above-normal rainfall years led to sustained recovery and gains that gradually accumulated in the regional water budget. This notwithstanding, projected drought intensification and increasing aridity due to climate change could heighten water stress in the region if robust water-resources management measures are not implemented to harness groundwater in a way that complements surface water sources.

Our analysis showed a connection between rainfall and groundwater storage at the well scale, and aquifer systems operating across multiple temporal scales. Deeper aquifers such as Nadapal-IRC and Kalobeyei provide delayed but substantial recharge, sustaining water availability for extended periods. Shallower systems at Kakemera and Loturerei recharge more slowly and are likely more vulnerable to seasonal drought. This differentiated recharge behavior underscores the need for localized groundwater management approaches that reflect both recharge dynamics when designing monitoring networks, abstraction regimes, and drought-adaptation strategies across the study domain. The observed spatial and temporal patterns carry significant implications for water-resource management and climate adaptation in the region. Seasonal rainfall extremes and their influence on water systems in the region reflect a regime in which water security increasingly depends on capturing intense rainfall events. The heterogeneous groundwater responses necessitate localized adaptation strategies that account for both the immediate vulnerability of rapid-response systems and the long-term vulnerability of slow-response systems. Furthermore, the regional groundwater-storage patterns and their evident relationship with anomalous rainfall underscore the importance of considering extended hydrological cycles in water-resource planning, as the impacts of drought or surplus conditions persist long after individual rainfall seasons. Such a comprehensive understanding of rainfall–storage relationships across spatial and temporal scales would provide a critical foundation for developing resilient water-management strategies in this vulnerable region.

These findings carry significance beyond the Turkana region. Africa's drylands have biophysical similarities with the study domain. These regions are faced with increasing water insecurity due to intensifying climate change impacts, population growth, rising water demand, and environmental degradation. Highly variable surface water in the drylands – often where exploitation is focused – has led to increased attention on the potential of groundwater to ameliorate water stress. This attention is supported by recent research showing groundwater storage in these regions to be more than 100 times that of renewable freshwater storage [44], offering evidence that this resource offers a foundation for development. Whereas there is also concern about the expansion of water infrastructure in the African drylands and the impacts this might have on existing climate change adaptation practices [14], mostly due to poorly governed water development, a shift towards increased groundwater exploitation and sustainable management can buffer the pastoral dryland communities from persistent water insecurity, and in turn, strengthen their resilience to climate impacts [45]. Ultimately, the sustainability of groundwater aquifers in the region will depend on a comprehensive understanding of the factors that contribute to healthy aquifers which should include a combination of site-level and regional management practices.

Considerations for future research

This study successfully characterized the dynamic balance between aquifer drawdown and recovery and the interaction between rainfall and terrestrial water storage. However, the analysis remains constrained by its methodological framework. The findings were derived primarily from statistical interpretations of groundwater hydrographs, and complementary remote-sensing observations and model products. While these approaches are powerful for detecting local and regional patterns and establishing correlative relationships, they provide limited capacity to quantify aquifer properties or reveal the physical processes controlling hydrological responses. Consequently, although differential aquifer behaviors were evident across the study domain, there is little knowledge about the underlying hydrogeological mechanisms such as recharge efficiency, storage capacity, and hydraulic connectivity. A central limitation is the absence of robust ground-truth data to support detailed water-resource assessments. Only a few monitoring wells exist in the region, and, to the best of our knowledge, no other continuous datasets are available to characterize groundwater–rainfall relationships beyond those used in this study.

To address these gaps, future research should prioritize targeted, field-based aquifer characterization through a network of long-term monitoring stations distributed across the region. These efforts must be complemented by systematic aquifer pumping tests – currently limited, outdated, or unreliable – to quantify essential hydraulic parameters. Integrating these empirical datasets into numerical groundwater models would enable simulation of climate variability and abstraction impacts, thereby informing sustainable water management and allocation. Given ongoing and planned water-development initiatives, such evidence-based frameworks could transform groundwater governance from reactive and ad hoc to proactive and data-driven. Already, the World Bank has invested USD 385 million in groundwater development across the Horn of Africa [46], with initiatives aimed at strengthening drought resilience through improved aquifer characterization and monitoring. This regional program supports the mapping of transboundary and seasonal aquifers that experience seasonal recharge across Ethiopia, Kenya, and Somalia, and are therefore more prone to climate risks, providing critical evidence to guide sustainable groundwater use and management in these data-scarce drylands. Integrating water quality assessments and improvement into these efforts must also be recognized as integral to broader water security goals. In regions with limited sanitation infrastructure and widespread pastoral activity, microbial contamination poses serious health risks. Therefore, achieving long-term water security will require that future programs embed water-quality improvements as a core component of groundwater development and management interventions.

Conclusion

This study examined the groundwater dynamics of the Turkana region in arid northern Kenya by integrating seasonal rainfall analysis, GRACE-derived terrestrial water storage, GLDAS-modeled groundwater storage, and site-level groundwater monitoring. The analysis revealed a clear climate signal in regional water storage, characterized by pronounced interannual variability driven by alternating drought and wet extremes across the MAM and OND seasons. The OND season showed a progressive shift toward wetter conditions over the study period, while MAM rains experienced episodic wet anomalies. These rainfall extremes exerted a notable influence on groundwater storage, with GLDAS CLSM-modeled annual mean groundwater volume increasing by approximately 21.7% between 2004 and 2024, from 109.68 km^3 to 133.49 km^3, punctuated by substantial declines during consecutive drought episodes between 2020 and 2023. Site-level monitoring corroborated these regional patterns, revealing near-balanced drawdown–recovery dynamics likely from sustained net groundwater storage after the 2019-2020 events and subsequent high rainfall events in 2023 and 2024. In addition, we found site-specific recovery lags associated with rainfall accumulation ranging from approximately one to four months, reflecting the heterogeneity of aquifer systems across the study region.

Our findings underscore the strong sensitivity of groundwater systems in this region to rainfall events and highlight both the opportunity and urgency of sustainable groundwater management in East African drylands. Rapid-response aquifer systems offer immediate relief during drought but remain vulnerable to prolonged dry spells, while slower-recharging systems provide more sustained storage but require longer recovery periods following depletion. These contrasting behaviors necessitate localized, evidence-based management strategies that account for recharge dynamics, abstraction regimes, and projected intensification of climate variability. The broader relevance of these findings extends to dryland regions across Africa where groundwater represents a critical but undercharacterized buffer against growing water insecurity. Realizing the full potential of this resource will require sustained investment in aquifer characterization, long-term monitoring networks, and integrated numerical modeling frameworks that can translate climate signals into actionable guidance for water governance and drought adaptation.

Acknowledgments

The authors acknowledge the contributions of field technicians who installed and maintained the water-level sensor network, including Virridy's field technician, Newton Kiriungi, and the many individuals from local communities who provided additional context for characterizing the study sites.

This manuscript is submitted for publication with the understanding that the United States Government is authorized to reproduce and distribute reprints for Governmental purposes. The views and conclusions contained in this document are those of the authors and should not be interpreted as representing the opinions or policies of the U.S. Geological Survey. Mention of trade names or commercial products does not constitute their endorsement by the U.S. Geological Survey.

References

1. Thomas E, Needoba J, Kaberia D, Butterworth J, Adams EC, Oduor P, et al. Quantifying increased groundwater demand from prolonged drought in the East African Rift Valley. Science of The Total Environment. 2019;666:1265-72.

2. Thomas E, Jordan E, Linden K, Mogesse B, Hailu T, Jirma H, et al. Reducing drought emergencies in the Horn of Africa. Science of The Total Environment. 2020;727:138772. doi:10.1016/J.SCITOTENV.2020.138772.

3. Senay GB, Velpuri NM, Alemu H, Pervez SM, Asante KO, Karuki G, et al. Establishing an operational waterhole monitoring system using satellite data and hydrologic modelling: Application in the pastoral regions of East Africa. Pastoralism: Research, Policy and Practice. 2013;3:1-16. doi:10.1186/2041-7136-3-20.

4. Gebremeskel G, Tang Q, Sun S, Huang Z, Zhang X, Liu X. Droughts in East Africa: Causes, impacts and resilience. Earth-Science Reviews. 2019;193:146-61. doi:10.1016/j.earscirev.2019.04.015.

5. Famiglietti JS. The global groundwater crisis. Nature Climate Change. 2014 Nov;4(11):945-8. Available from: `https://doi.org/10.1038/nclimate2425`. doi:10.1038/nclimate2425.

6. Wada Y, Beek LPHV, Kempen CMV, Reckman JWTM, Vasak S, Bierkens MFP. Global depletion of groundwater resources. Geophysical Research Letters. 2010;37(20). doi:10.1029/2010GL044571.

7. Scanlon BR, Rateb A, Anyamba A, Kebede S, Macdonald AM, Shamsudduha M, et al. Linkages between GRACE water storage, hydrologic extremes, and climate teleconnections in major African aquifers. Environmental Research Letters. 2022;17(1). doi:10.1088/1748-9326/ac3bfc.

8. Fankhauser K, Macharia D, Coyle J, Kathuni S, McNally A, Slinski K, et al. Estimating groundwater use and demand in arid Kenya through assimilation of satellite data and in-situ sensors with machine learning toward drought early action. Science of the Total Environment. 2022;831:154453.

9. Wendt DE, Van Loon AF, Bloomfield JP, Hannah DM. Asymmetric impact of groundwater use on groundwater droughts. Hydrology and Earth System Sciences. 2020;24(10):4853-68. doi:10.5194/hess-24-4853-2020.

10. Van Loon AF, Rangecroft S, Coxon G, Naranjo JAB, Van Ogtrop F, Van Lanen HAJ. Using paired catchments to quantify the human influence on hydrological droughts. Hydrology and Earth System Sciences. 2019;23(3):1725-39. doi:10.5194/hess-23-1725-2019.

11. Rohde MM, Albano CM, Huggins X, Klausmeyer KR, Morton C, Sharman A, et al. Groundwater-dependent ecosystem map exposes global dryland protection needs. Nature. 2024;632(8023):101-7. doi:10.1038/s41586-024-07702-8.

12. Thatch LM, Gilbert JM, Maxwell RM. Integrated Hydrologic Modeling to Untangle the Impacts of Water Management During Drought. Groundwater. 2020;58(3):377-91. doi:10.1111/gwat.12995.

13. Thomson P, Bradley D, Katilu A, Katuva J, Lanzoni M, Koehler J, et al. Rainfall and groundwater use in rural Kenya. Science of the Total Environment. 2019;649:722-30. doi:10.1016/j.scitotenv.2018.08.330.

14. Piemontese L, Terzi S, Di Baldassarre G, Menestrey Schwieger DA, Castelli G, Bresci E. Over-reliance on water infrastructure can hinder climate resilience in pastoral drylands. Nature Climate Change. 2024;14(3):267-74. doi:10.1038/s41558-024-01929-z.

15. Opiyo F, Nyangito M, Wasonga OV, Omondi P. Trend Analysis of Rainfall and Temperature Variability in Arid Environment of Turkana, Kenya. Environmental Research Journal. 2014;8(2):30-43.

16. Bauman P, Ernst E, Woods L. Surface geophysical exploration for groundwater at the Kakuma refugee camp in Turkana County, Kenya. CSEG Recorder. 2017;42:36-43.

17. Tanui F, Olago D, Dulo S, Ouma G, Kuria Z. Hydrogeochemistry of a strategic alluvial aquifer system in a semi-arid setting and its implications for potable urban water supply: The Lodwar Alluvial Aquifer System (LAAS). Groundwater for Sustainable Development. 2020;11:100451. doi:https://doi.org/10.1016/j.gsd.2020.100451.

18. Maidment RI, Grimes D, Allan RP, Tarnavsky E, Marcstringer M, Hewison T, et al. The 30 year TAMSAT african rainfall climatology and time series (TARCAT) data set. Journal of Geophysical Research. 2014;119(18):10, 619-0, 644. doi:10.1002/2014JD021927.

19. Maidment RI, Grimes D, Black E, Tarnavsky E, Young M, Greatrex H, et al. A new, long-term daily satellite-based rainfall dataset for operational monitoring in Africa. Scientific Data. 2017;4:1-2. doi:10.1038/sdata.2017.63.

20. Tarnavsky E, Grimes D, Maidment R, Black E, Allan RP, Stringer M, et al. Extension of the TAMSAT satellite-based rainfall monitoring over Africa and from 1983 to present. Journal of Applied Meteorology and Climatology. 2014;53(12):2805-22. doi:10.1175/JAMC-D-14-0016.1.

21. Blumenthal MB, Bell M, del Corral J, Cousin R, Khomyakov I. IRI Data Library: enhancing accessibility of climate knowledge. Earth Perspectives. 2014;1(1):19.

22. Macharia D, Fankhauser K, Selker JS, Neff JC, Thomas EA. Validation and intercomparison of satellite-based rainfall products over Africa with TAHMO in situ rainfall observations. Journal of Hydrometeorology. 2022;23(7):1131-54.

23. Watkins MM, Wiese DN, Yuan DN, Boening C, Landerer FW. Improved methods for observing Earth's time variable mass distribution with GRACE using spherical cap mascons. Journal of Geophysical Research: Solid Earth. 2015;120(4):2648-71.

24. Adloff M, Singer MB, MacLeod DA, Michaelides K, Mehrnegar N, Hansford E, et al. Sustained Water Storage in Horn of Africa Drylands Dominated by Seasonal Rainfall Extremes. Geophysical Research Letters. 2022;49(21). doi:10.1029/2022GL099299.

25. Ferreira VG, Yang H, Ndehedehe C, Wang H, Ge Y, Xu J, et al. Estimating groundwater recharge across Africa during 2003–2023 using GRACE-derived groundwater storage changes. Journal of Hydrology: Regional Studies. 2024;56:102046. doi:10.1016/j.ejrh.2024.102046.

26. Bonsor HC, Shamsudduha M, Marchant BP, MacDonald AM, Taylor RG. Seasonal and decadal groundwater changes in African sedimentary aquifers estimated using GRACE products and LSMs. Remote Sensing. 2018;10(6). doi:10.3390/rs10060904.

27. Sun AY, Green R, Swenson S, Rodell M. Toward calibration of regional groundwater models using GRACE data. Journal of Hydrology. 2012;422-423:1-9. doi:10.1016/j.jhydrol.2011.10.025.

28. Li B, Rodell M, Kumar S, Beaudoing HK, Getirana A, Zaitchik BF, et al. Global GRACE Data Assimilation for Groundwater and Drought Monitoring: Advances and Challenges. Water Resources Research. 2019;55(9):7564-86. doi:10.1029/2018WR024618.

29. R Core Team. R: A language and environment for statistical computing. R Foundation for Statistical Computing, Vienna, Austria. http://www R-project org/. 2016.

30. Schulzweida U, Kronblueh L, Budich RG. CDO: Climate Data Operators. Accessed: Apr. 2019;8:2024.

31. Entekhabi D. Propagation in the drought cascade: observational analysis over the continental US. Water Resources Research. 2023;59(9):e2022WR032608.

32. Amazirh A, Chehbouni A, Bouras EH, Benkirane M, Hssaine BA, Entekhabi D. Drought cascade lag time estimation across Africa based on remote sensing of hydrological cycle components. Advances in Water Resources. 2023 Dec;182:104586. Available from: `https://www.sciencedirect.com/science/article/pii/S0309170823002208`. doi:10.1016/j.advwatres.2023.104586.

33. McKee TB, Doesken NJ, Kleist J. The relationship of drought frequency and duration to time scales. In: Proceedings of the 8th Conference on Applied Climatology. vol. 17. Boston; 1993. p. 179-83.

34. Bloomfield JP, Marchant BP. Analysis of groundwater drought building on the standardised precipitation index approach. Hydrology and Earth System Sciences. 2013;17(12):4769-87. Available from: `https://hess.copernicus.org/articles/17/4769/2013/`. doi:10.5194/hess-17-4769-2013.

35. Funk C, Dettinger MD, Michaelsen JC, Verdin JP, Brown ME, Barlow M, et al. Warming of the Indian Ocean threatens eastern and southern African food security but could be mitigated by agricultural development. Proceedings of the national academy of sciences. 2008;105(32):11081-6.

36. Nicholson SE. Climate and climatic variability of rainfall over eastern Africa. Reviews of Geophysics. 2017;55(3):590-635. doi:https://doi.org/10.1002/2016RG000544.

37. Dutra E, Magnusson L, Wetterhall F, Cloke HL, Balsamo G, Boussetta S, et al. The 2010-2011 drought in the Horn of Africa in ECMWF reanalysis and seasonal forecast products. International Journal of Climatology. 2013;33(7):1720-9.

38. Wainwright CM, Finney DL, Kilavi M, Black E, Marsham JH. Extreme rainfall in East Africa, October 2019–January 2020 and context under future climate change. Weather. 2020.

39. Funk C, Fink AH, Harrison L, Segele Z, Endris HS, Galu G, et al. Frequent but Predictable Droughts in East Africa Driven by a Walker Circulation Intensification. Earth's Future. 2023;11(11). doi:10.1029/2022EF003454.

40. Yang W, Seager R, Cane MA, Lyon B. The East African Long Rains in Observations and Models. Journal of Climate. 2014;27(19):7185 7202. doi:10.1175/JCLI-D-13-00447.1.

41. Lyon B, DeWitt DG. A recent and abrupt decline in the East African long rains. Geophysical Research Letters. 2012;39(2). doi:https://doi.org/10.1029/2011GL050337.

42. Kimutai J, Barnes C, Zachariah M, Philip SY, Kew SF, Pinto I, et al. Human-induced climate change increased 2021–2022 drought severity in horn of Africa. Weather and Climate Extremes. 2025;47:100745. doi:10.1016/j.wace.2025.100745.

43. Tanui F. Characterization of the Hydrogeology of the Lodwar Alluvial Aquifer System, Turkana County, Kenya [PhD Thesis]. University of Nairobi; 2021.

44. MacDonald AM, Bonsor HC, Dochartaigh B\\, Taylor RG. Quantitative maps of groundwater resources in Africa. Environmental Research Letters. 2012;7(2):024009.

45. Cobbing J, Hiller B. Waking a sleeping giant: Realizing the potential of groundwater in Sub-Saharan Africa. World Development. 2019;122:597-613.

46. World Bank. Horn of Africa - Groundwater for Resilience Program. World Bank Group; 2025. Available from: https://projects.worldbank.org/en/projects-operations/project-detail/P174867.